Quantum dots for solar energy harvesting

Karen Das and Sunandan Baruah*

Department of ECE, School of Technology, Assam Don Bosco University, Azara, Guwahati 781 017, India

Owing to their versatile optical and electrical properties, semiconductor quantum dots are attracting attention as a material of choice for solar energy conversion. The quantum dot sensitized solar cells are considered as one of the most promising next-generation solar cells as they have the advantage of tunable band-gap energy and multiple exciton generation. We present here a study on quantum dot sensitized solar cells considering their construction and working, impact of incorporation of nanomaterials in solar cells and various structures for improving the performance of solar cells.

Keywords: Light harvesting, multiple exciton generation, quantum dots, solar cells, tunable band gap.

ENERGY generation in the modern era always had a problem in keeping pace with the increased demand of the ever burgeoning population. The world is changing; the standard of living of the people is resulting in rapid increase in the global consumption of energy (10 trillion kWh at present) and the US Energy Information Administration predicts global energy demand of 35 trillion kWh in 2035 (ref. 1). The amount of energy that is showered by the sun on the earth in an hour is enough to fulfil the global need of energy for a year[2]. The need of the hour, therefore, is some innovation that will provide electricity using the abundantly available solar energy at minimal expenses to support the base of the pyramid population.

As a cost-effective alternative to silicon-based photovoltaic systems, recently, quantum dot sensitized solar cells (QDSSCs) have gained considerable popularity. QDSSCs, an evolution from dye sensitized solar cells (DSSCs) which were first reported by O'Regan and Grätzel in 1991, are considered to have great potential as the next generation of solar cells (SCs). Several efforts have been made to obtain an ideal organic dye as a sensitizer to absorb photons in the full visible spectra. It has been a challenge to obtain such an ideal organic dye. Hence, narrow band-gap semiconductor quantum dots (QDs), such as CdSe, InAs, CdS and PbS became more popular as photosensitizers due to their versatile optical and electrical properties, such as higher stability towards oxygen and water, tuneable band gap depending on the

QD size, multiple exciton generation (MEG) with single-photon absorption and larger extinction coefficient[3,4].

Light absorption and exposure of the photon-sensitive material to light are the two main factors that govern the efficiency of a SC. Very high light absorption can be achieved using QDs adsorbed on nanostructured materials. Through tuning of the band gap of the QDs, absorption of various wavelengths of the visible spectrum of light can be achieved. Coupling QDs with semiconducting nanorods which have high surface area allows better tapping of sunlight as more photon-absorbing QDs can be coupled to the surface. The incorporation of nanomaterials improves photoenergy absorption owing to high available surface area. In this article, the impact of nanomaterials in QDSSCs and various possible structures for improving the performance of QDSSCs are presented.

Construction of QDSSCs

Figure 1 shows the typical construction schematic of QDSSC. It consists of a photoanode and a counter electrode separated by a redox couple[5,6]. The photoanode consists of a wide band gap, mesoporous semiconductor layer attached to conducting glass and QDs adsorbed onto the semiconductor layer. QDs work as sensitizer in which electron–hole pairs are created upon exposure to light. Mesoporous structure of the semiconducting layer provides enhanced surface-to-volume ratio, which in turn facilitates enhancement in the adsorption of QDs onto it. The redox couple scavenges the photogenerated holes and produces electrical equilibrium in the semiconducting layer. Sulphide/polysulphide redox couple is most widely used because of its higher open circuit voltage and better stability for photovoltaic operation[7,8]. Various additives have been explored with sulphide/polysulphide redox couple[9]. In fact, a new record of average power conversion efficiency of 12.3% of Zn–Cu–In–Se QD-based QDSSCs has been reported[9], where 6 vol% tetraethyl orthosilicate is used as an additive in polysulphide electrolyte. $CdS^{10,11}$, $CdSe^{12,13}$, $ZnSe^{14,15}$, $PbS^{16,17}$, $Ag_2S^{18,19}$, $CuInS_2^{20,21}$, $CdTe^{22,23}$, $InP^{24,25}$ and $CdHgTe^{26,27}$ are materials of choice for QDs to be used as sensitizer in QDSSC design. The most popularly used wide band gap semiconductor in QDSSCs is TiO_2 (ref. 28). ZnO, SnO_2 and Nb_2O_5 are also reported to be used as mesoporous semiconducting layer in QDSSCs[29–31].

---

*For correspondence. (e-mail: sunandan.baruah@dbuniversity.ac.in)
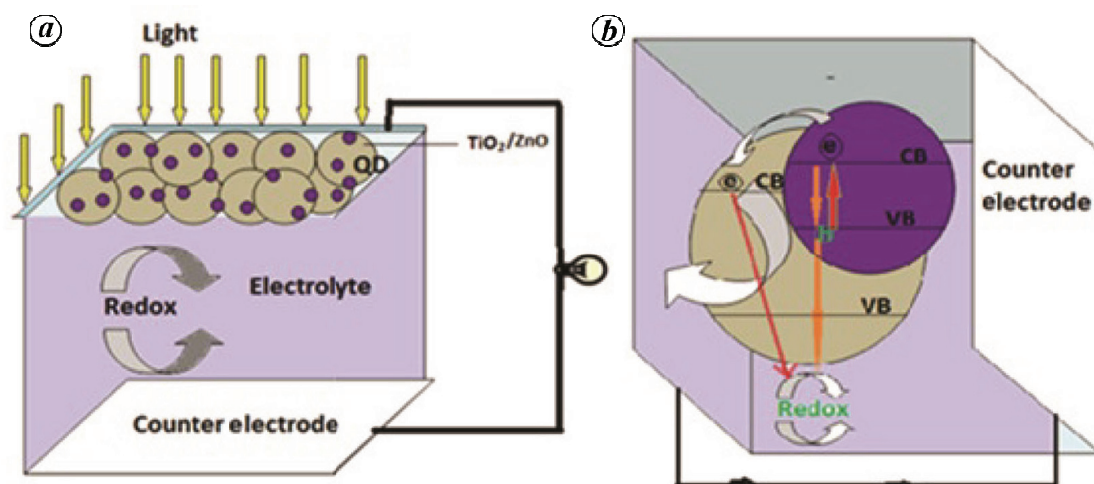
Figure 1. *a*, Complete set-up of quantum dot sensitized solar cell. *b*, Single nanoparticle with an adsorbed quantum dot (QD) showing the energy bands.

Liu et al.[32] used TiO_2 as wide band gap semiconductor and CdS/CdSe QDs as sensitizer with application of SiO_2 coating using successive ion layer adsorption and reaction (SILAR) and chemical bath deposition (CBD) method, and achieved a fill factor (FF) of 41% and efficiency of 2.05%. Seol et al.[33] reported FF of 38.3% and efficiency of 4.15%, when they covered ZnO nanorods by CdS shells to reduce the charge recombination and CdSe QDs were utilized as sensitizer using CBD method. Yu et al.[34] reported a QDSSC design using CdS/CdSe QDs as sensitizer, TiO_2 as wide band gap semiconductor and Cu_2S in counter electrode using CBD method and achieved efficiency of 4% and FF of 60.1%. Fang et al.[35] using carbon nanofibres as counter electrode, CdSe QDs as sensitizer and TiO_2 as wide band gap semiconductor achieved FF of 60% and efficiency of 4.81%. Radich et al.[36] prepared SILAR method based QDSSCs using CdS/CdSe as sensitizer and TiO_2 as wide band gap semiconductor and got FF of 46% and efficiency of 4.4%. Zhang et al.[37] reported FF of 63% and efficiency of 4.92% using larger sized TiO_2 as wide band gap semiconductor and CdS/CdSe as sensitizer. Hossain et al.[38] reported FF of 57% and efficiency of 5.21%. They used CdSe QD as sensitizer and TiO_2 as wide band gap semiconductor with a buffer layer of CdS following the SILAR method. Santra and Kamat[39] also used the SILAR method to prepare QDSSCs, and achieved FF of 47% and efficiency of 5.42% when they used Mn-doped CdS/CdSe and TiO_2.

Zinc oxide with a direct band gap of 3.37 eV is also gaining attention along with TiO_2, which has been the most sought after for DSSC photoelectrodes[40]. The advantage of using ZnO over TiO_2 is its direct band gap (TiO_2 has an indirect band gap of 3 eV) and high exciton binding energy of 60 meV (refs 41, 42). ZnO also has a higher electron mobility (200 cm^2/V/s) than TiO_2

(30 cm^2/V/s), which makes it a better choice than TiO_2 (ref. 43). Another advantage of ZnO is that it has the largest collection of nanostructures ever recorded like nanorods/nanowires, hierarchical nanostructures, nanosheets, nanoneedles, nanotubes, etc. By controlling the structure of single crystalline ZnO, it is possible to reduce electron hopping and enhance electron mobility. The single crystalline ZnO nanorods provide a direct path for the diffusion of electrons through them. Further, densely grown ZnO nanorod arrays can provide a very high surface area compared to volume. ZnO nanorods can be grown using simple hydrothermal methods[44], making them the most suitable for low-cost QDSSC design. Numerous reports are also available on the use of ZnO nanostructures in QDSSC[45–47]. However, the reported efficiency of ZnO-based DSSCs is still lower than the TiO_2-based ones.

Impact of nanomaterials in QDSSCs

Incorporation of QDs in SCs is advantageous as it provides higher stability towards oxygen and water, tuneable band gap depending on size, multiple exciton generation with single-photon absorption, larger extinction coefficient and low cost.

Among these, band gap tenability and multiple exciton generation are gaining importance as they have a direct impact on photon absorption and photocurrent generation.

Tunable band gap

Band gap of QDs can be tuned by varying their size owing to quantum confinement phenomenon in nanometre scale[48,49], which leads to size-dependent optical properties of QDs. This is advantageous for controlled

light energy harvesting. CdS[50] and CdSe[51–53] QDs have been reported quite often for tunable band gap. With decrease in the size of QDs, the effective band gap energy increases. As a result, light absorption and emission shift towards higher energies. Blue shift in the optical spectra of CdSe[54] and CdS[55] QDs with decrease in size has been reported. Photocurrent increases with decrease in QD size owing to the shift of conduction band towards more negative potential, which in turn improves the condition for charge injection. On the contrary, with increase in the size of QDs, better absorption in the visible region is observed. However, smaller sizes have better electron injection into the transporting layer than the bigger ones. A demonstration of size-based optimization of efficient charge separation can be found in Vogel et al.[56]. Improved photoelectrochemical response and photoconversion efficiency have been reported by Kongkanand et al.[52] by varying the size of CdSe QDs. So a combination of different sized ODs must improve the photon absorption scenario, which will definitely improve the efficiency of SCs. Figure 2 is a schematic of photoanode which will absorb the entire visible spectrum; hence it can be termed as photoanode of rainbow SC.

Multiple exciton generation

If a photon with energy greater than the bandgap (E_g) of a semiconductor is incident on it, then the energy in excess
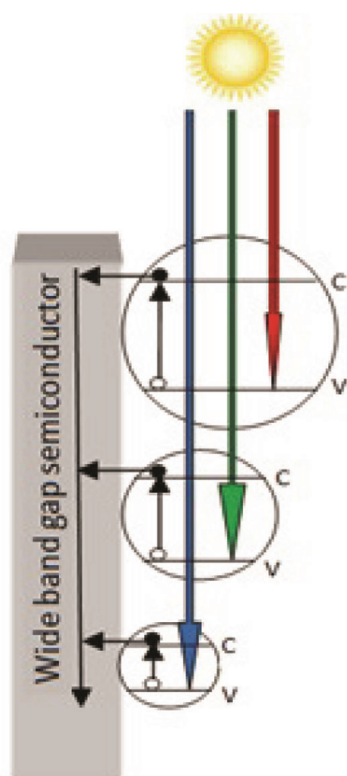
Figure 2. Schematic structure of photoanode of a rainbow solar cell.

of E_g gets lost after generating a single exciton. Based on this assumption, the maximum thermodynamic conversion in SCs is observed to be 43.9% (ref. 57).

This thermodynamics conversion limitation can be overcome by harnessing the carrier multiplication of the cells[58–60], which is considered an attractive technique to improve solar energy conversion. Carrier multiplication can be achieved in nano semiconductor crystals through impact ionization, a kind of inverse Auger process, where an exciton generated in a semiconductor by absorption of photo-energy greater than $2E_g$ relaxes by energy transfer of at least $1E_g$ to the band edge, thereby generating another exciton[61]. To increase the solar energy conversion through carrier multiplication, the rate of impact ionization has to be greater than the exciton relaxation by means of emission of phonons. The relaxation dynamics is largely affected by quantization effect, which can be produced in a semiconductor by dint of quantum confinement[62–64]. When the size of the nanosemiconductor crystals is comparable to Bohr radius, the rate of impact ionization increases extensively and becomes comparable to the rate of cooling of the hot carriers. Schaller and Klimov[57] carried out a detailed study on carrier multiplication in PbSe nanocrystals through impact ionization. Figure 3 a shows the generation of biexcitaton. In the Auger process, two excitons recombine and produce highly energetic single excitons (Figure 3 b). Figure 3 c shows the immediate consequences of high photon excitation ($h\omega/E_g > 3$); initially high-energy excitons form in nano semiconducting crystals and then some (n_{xx}) of the excitons go through impact ionization and produce biexcitons while some (n_x) simply relax to the band edge and remain as single excitons and with time biexcitons go through the Auger process and produce single excitons. The change in population of exciton for low pump photon energies shows a step function with time while those with high energies exhibit an exponentially decaying function (Figure 3 d).

Structures of QDSSCs

Apart from the structure discussed earlier in the text, many structures of SCs have been evolved based on QD sensitizers. Among them tandem SCs, core-shell SCs and plasmonic SCs have been able to draw the attention of researchers.

Tandem solar cells

The tandem SCs simultaneously address two key problems of SCs, viz. energy loss due to thermalization of hot charge carriers and sub-band gap transmission. It was reported that stacking multiple sub-cells in series can provide theoretical efficiency more than that of the Shockley–Queisser limitation[65]. With increase in the
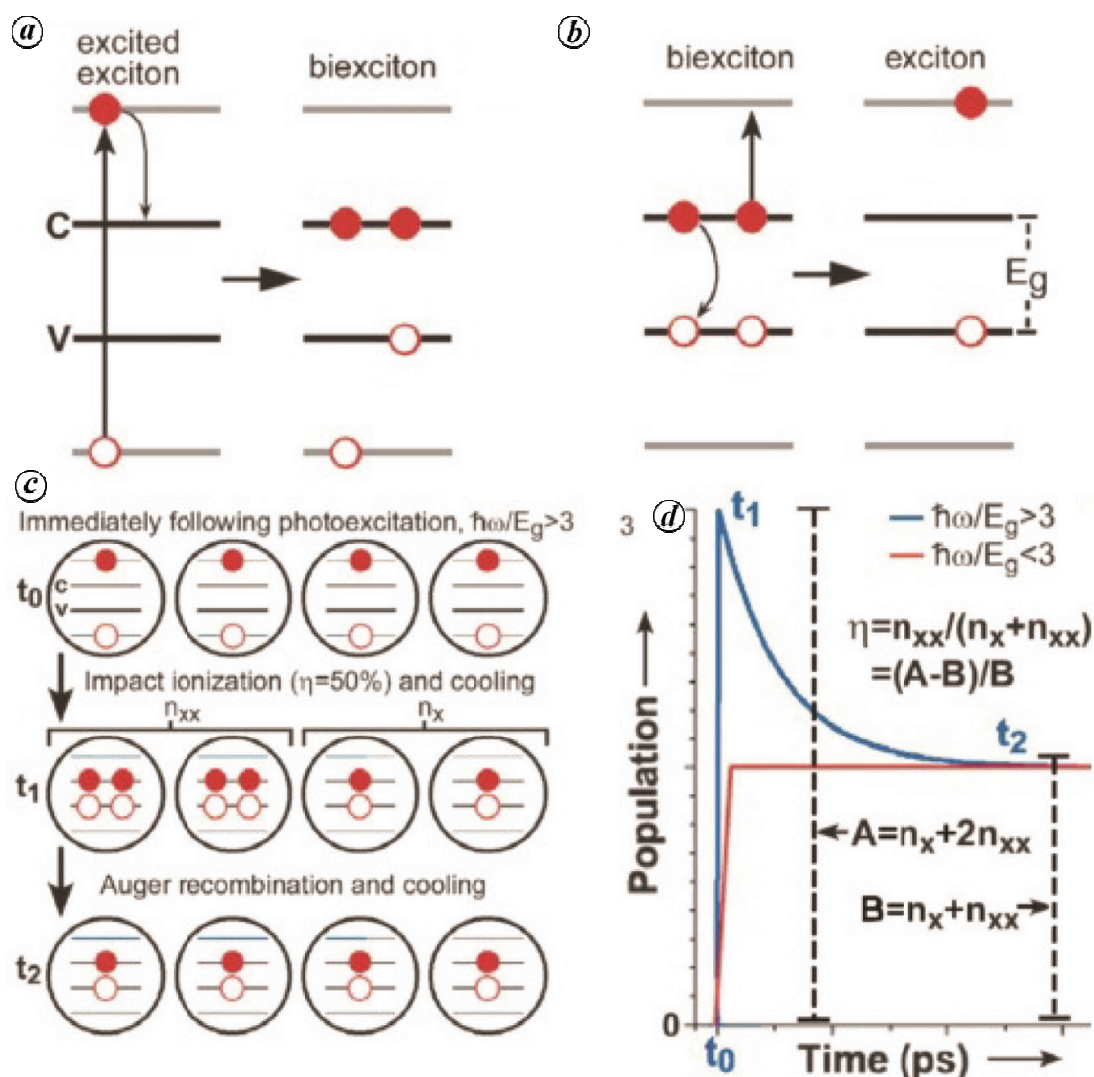
Figure 3. Demonstration of multiple excitation generation in QDSSCs (adapted from ref. 57). *a*, Impact ionization; *b*, auger process; *c*, dynamic carrier population; *d*, change in population with time.

number of sub-cells, efficiency increases and the maximum efficiency possible with infinite number of sub-cells is 68% (ref. 66). Figure 4 *a* shows the structure of a typical tandem SC. It comprises two (or more) independent sub-cells stacked on top of one another, which are based on acceptor–donor composite. The part of the wavelength not absorbed in the top sub-cell will impinge further to the bottom sub-cell. So the absorption spectra for both the sub-cells will be different as (Figure 4 *b*). Materials of unlike band gaps are used to reduce the thermalization loss. The intermediate layer needs to provide a platform for the recombination of electrons that are coming from one sub-cell with that of holes coming from the other sub-cell. This is precisely why this layer is also called the recombination layer. The materials for intermediate layer need to be selected to ensure that the quasi-Fermi level of the acceptor of the top sub-cell is aligned with that of the donor of the bottom sub-cell (Figure 4 *c*) or vice-versa. A

very thin layer of Ag (ref. 67), or Au (ref. 68) is reported to be used as the intermediate layer. The intermediate layer is decomposed into two layers, one layer made of *p*-type material, just under the top sub-cell to transport holes and the other layer made of *n*-type material, just above the bottom sub-cell to transport electrons[69]. At the interface of the *p*- and *n*-type materials, recombination of holes and electrons will take place.

If V_{OC1} and V_{OC2} are the open circuit voltages of sub-cells 1 and 2 respectively, then ideally the total open circuit voltage of the tandem SCs will be

$$V_{\text{Tandem}} = V_{OC1} + V_{OV2}.$$

In general,

$$V_{\text{Tandem}} = V_{OC1} + V_{OV2} + V_{OC3} + \cdots.$$

If I_{SC1} and I_{SC2} are the short circuit current of sub-cells 1 and 2 respectively, then the total short circuit current of the tandem SCs will be

$$I_{SC} = \min(I_{SC1}, I_{SC2}).$$

In general,

$$I_{SC} = \min(I_{SC1}, I_{SC2}, I_{SC3} \cdots).$$

However, a tandem cell (shown in Figure 4) is not feasible using liquid electrolyte and hence, as an alternative, use of tandem semiconducting layers in the photoanode is reported[70,71]. In a study by Santra and Kamat[70], three layers of CdSeS QDs of varying band gap were deposited in tandem using electrophoretic deposition method to the TiO₂-based photoanode of the QDSSC. Power conversion efficiency was reported to increase up to 1.97–2.81% compared to single-layer CdSeS. The authors[70] also reported that in two- and three-layered tandem QDSSCs, the maximum power conversion efficiencies were observed to be 3.2% and 3.0% respectively, which is greater than the three individually layered photoanodes. In another study by Lee et al.[71], a passivation layer of Cu–ZnS was deposited in tandem with TiO₂/CdS layer to enhance light harvesting as well as suppress the surface charge recombination. A tandem structure of TiO₂/CdS/Cu–ZnS was reported to have an improved efficiency of 3.35%, which is 82% higher than TiO₂/CdS-based QDSSCs (ref. 71).

Vitoreti et al.[72] studied two different semiconducting protective layers (CdS and ZnS) in CdTe-based Q-DSSCs. The ZnS layer can reduce recombination losses with the electrolyte; however, it can also disturb the charge-transfer mechanism. So the thickness of the layer has to be optimum; if it is very thick, the redox couple may be prohibited from reaching the QDs, causing a decrease in the efficiency of the cell. The authors[72] reported a reduction of 60% with ZnS layer covering CdTe QDs on TiO₂, when compared to the uncovered CdTe. However, use of CdS layer as passivation of the surface of the adsorbed QDs is reported to have 350% increase in cell efficiency, but cell stability is hampered. Vitoreti et al.[72] also studied double layer passivation with both CdS and ZnS in tandem. Cell efficiency was reported to increase by 600% with double layer of passivation compared to the cells containing only CdTe. The authors[72] proposed that CdS layer increases the absorption range and ZnS layer reduces the recombination losses with the electrolyte.

Core-shell solar cell

Figure 5 shows the structure of a core–shell SC, where PbS quantum dot is at the core which is covered by CdS
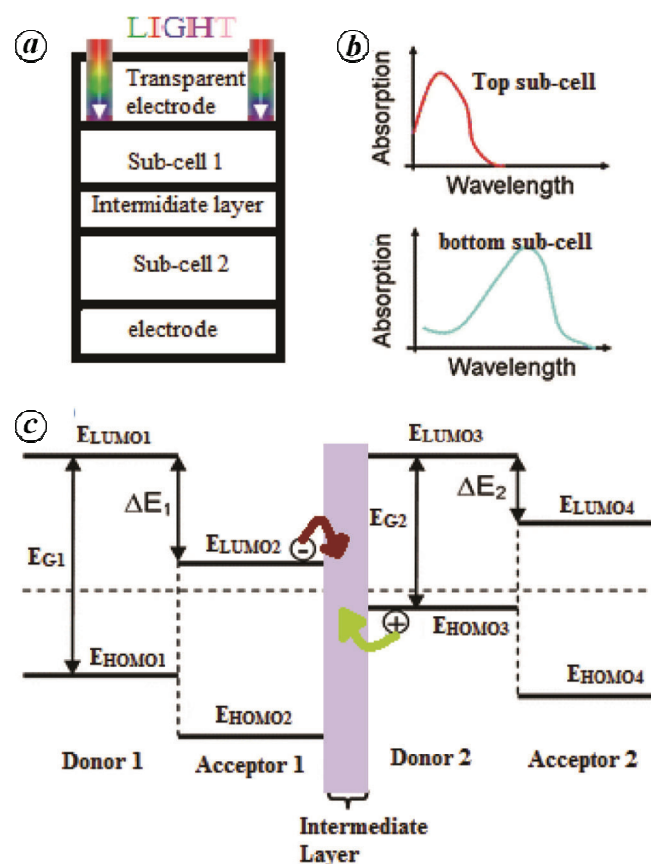
Figure 4. Tandem solar cell: *a*, structure; *b*, absorption of its two sub-cells; *c*, charge transport in tandem SCs.
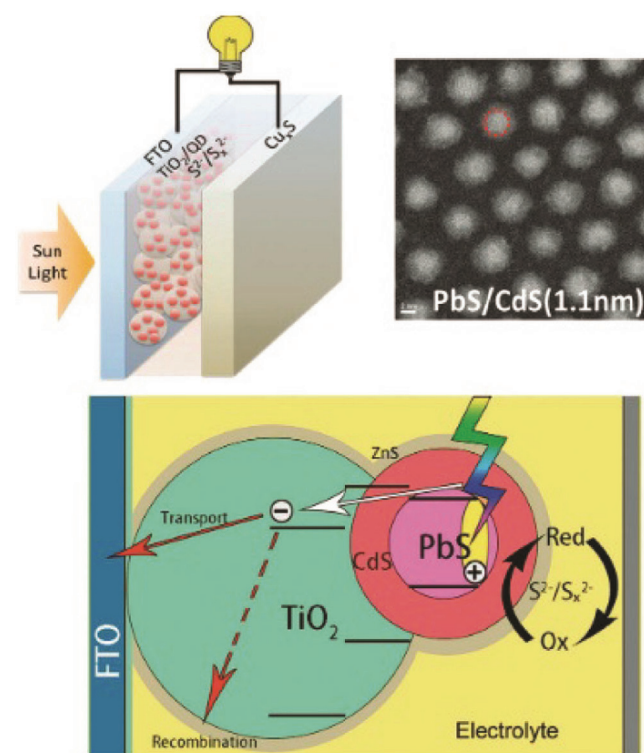
Figure 5. Structure of core–shell based QDSSC (reproduced from ref. 75).
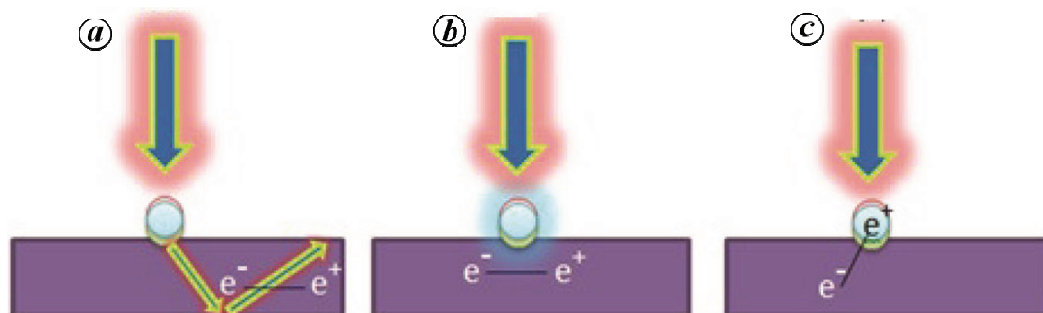
Figure 6. Demonstration of plasmonic effect in SCs.

shell. The ZnS coating gives twofold advantage of having the effect of blocking electrons[73], which possibly will recombine with the electrolyte, and coating defect states that may trap carriers[74].

Even though a typical SC absorbs a wide band of the solar spectrum, most of the absorbed energy is lost by rapid cooling of the hot carriers. In core–shell structure, cooling of the hot carriers is slower. When the shell is sufficiently thick, the lower energy holes are confined to the core and higher energy holes primarily stay in the shell itself, which leads to the electronic decoupling of higher and lower-energy holes. This is the reason for slow cooling of hot carriers in the core–shell structure, which helps in carrier multiplication. A photo-generated hot hole in the shell collides with a valence band electron of the core, exciting it to cross the band gap, which generates a second electron–hole pair. Lai et al.[75] studied PbS core and CdS shell and found four times higher efficiency than what is obtained with simple PbS QDs coated with ZnS after deposition. Selopal et al.[76] conducted a study keeping the core size of CdSe/CdS-based core–shell solar cells fixed at 1.65 nm and varying the thickness of CdS shell. A maximum photoconversion efficiency of 3.01% was reported at a shell thickness of $\approx$1.96 nm. It was also reported that a favourable stepwise electronic band alignment for better electron transfer rate can be achieved by introducing a $CdSe_xS_{1-x}$ interfacial alloyed layer between CdSe core and CdS shell. $CdSe/(CdSe_xS_{1-x})_5/(CdS)_1$ core/shell QD-based QDSSCs are reported to have the maximum photoconversion efficiency of 6.86% (ref. 76).

Plasmonic solar cells

For higher absorption, design of SCs demands a thicker structure and for higher carrier collection, the demand is a thinner structure. Thickness of the SCs is therefore a vital parameter to be optimized. It is highly desirable to have an optically thick but physically thin structure of a SC, which can be achieved by plasmonic SCs where light trapping mechanism is introduced in already designed cells. Trapping can produce comparatively higher intensity of light at the surface of the sensitizer, which in turn leads to higher absorption and hence greater generation of electron–hole pairs.

The phenomenon of plasmon resonance increases the absorption of light into the SCs mainly by the following three ways.

1. By scattering light into the SCs, thereby increasing path length and hence absorption. When plasmonic nanoparticles scatter light at resonance frequency, they lead to a prolonged path of light compared to the non-scattered one. If the surrounding medium is homogeneous, then scattering takes place uniformly in both forward and backward directions. On the contrary, if the surrounding medium is inhomogeneous, then light is scattered preferably into the medium with higher dielectric constant. That is the case when metal nanoparticles are placed on top of the SC (Figure 6 a), with air (or any medium with lower dielectric constant) as surrounding medium. Scattered light gets trapped inside the SCs, if scattering takes place at an angle larger than the critical angle of the interface. This trapped light acts as a waveguide inside the cells, leading to prolonged path length and hence absorption by the cells. It also leads to higher current density in both thin and thick cells on index-matched substrates. This mechanism is influenced by the size of the nanoparticles. Larger nanoparticles result in increase of scattering efficiency, while smaller ones are preferred for scattering light more in the forward direction. This trade-off is overcome by placing the nanoparticles at the rear end between the glass substrate and transparent conductive layer. Moreover, plasmonic nanoparticles placed at the rear end help to excite propagating waveguide mode within the absorbing layer. This can lead to propagation of light either in surface plasmon polariton mode or photonic waveguide mode. In either cases, light is guided along the lateral direction of SCs, which in turn increases the path length and hence improves absorbance[77,78].

2. Absorption enhancement due to intensified near field around the plasmonic nanoparticle. It is known that the probability of electron excitation is proportional to the electric field[79]. Thus, an intensified electric field around
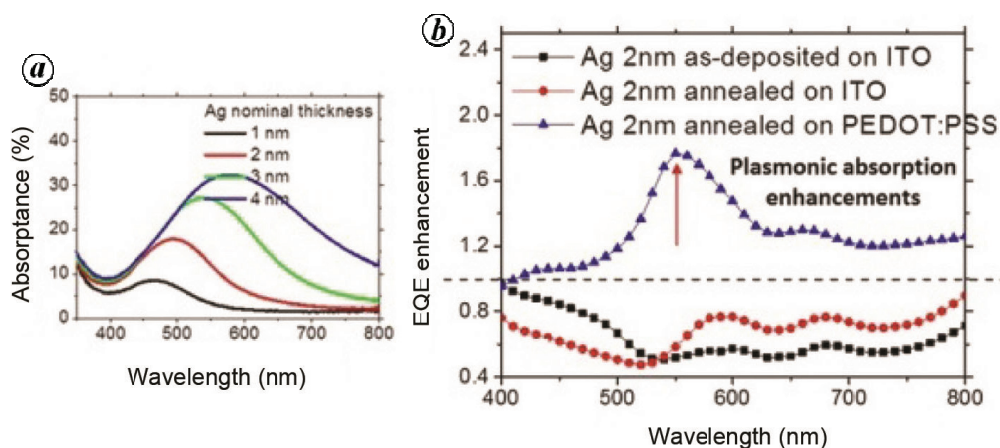
Figure 7. *a*, Optical absorptance of Ag nanoparticles on ITO glass. *b*, External quantum efficiency enhancement of SCs via introduction of Ag nanoparticles (reproduced from ref. 86).

plasmonic nanoparticles (Figure 6 *b*) results in enhanced excitation in the surrounding semiconductor and can store light energy as plasmon oscillation. Optical absorption is also proportional to the electric field. So a high electric field always results in increased absorption. Coupling of this energy into the surrounding semiconductor is possible only if the absorption coefficient of the semiconductor is greater than the inelastic plasmon decay time; otherwise the incident light energy will be absorbed in the plasmonic nanoparticles. This theory has been proved by Hägglund and co-workers[80–82]. This phenomenon is largely influenced by the shape and size of the plasmonic nanoparticles, metal–semiconductor interface, surface roughness of the metal and presence of metal oxide layer.

3. Decay of plasmon resonance by exciting electron–hole pair in the metal nanoparticles. Excitation of electron-hole pair in the metal nanoparticles takes place when the plasmon resonance decays (Figure 6 *c*). If the nanoparticle work function and semiconductor conduction band are properly aligned, then the electron generated can be transferred to the semiconductor, thus leaving the plasmonic nanoparticle charged. This can cause an increase in the short circuit current of the SC, if the nanoparticles are not electrically isolated from it, and thus leads to enhancement in the performance of SCs[83,84]. It is established that based on charge injection generated by plasmonic decay, efficiencies up to 7% can be achieved[85] when injection is through a Schottky barrier formed between the metal nanoparticle and semiconductor[85]. On the other hand, because of the broad distribution of energy, many of the excited electrons might not have sufficient energy to overcome the Scottky barrier as metals have high density of unoccupied energy states above the Fermi energy. However, if barrier is small, a reverse current flows from the semiconductor to the metal particle, which might contribute towards lowering the efficiency of SCs.

Figure 7 *a* shows the impact of incorporation of Ag nanoparticles in absorptance. Fleetham *et al.*[86] studied organic SC with Ag nanoparticles as plasmonic material and found that bigger size of metal nanoparticles is better for predominant scattering. They also found that incorporating a buffer layer of PEDOT : PSS between the ITO and the metal nanoparticles is better in the context to efficiency of the SCs, compared to direct adsorption of metal nanoparticles on ITO (Figure 7 *b*). The maximum external quantum efficiency was enhanced in the scale of 2.1 if optimum nanoparticles size was incorporated with the cell and 30% increase in photocurrent was achieved. To have greater absorption enhancement, Fleetham *et al.*[86] suggested incorporation of Ag nanoparties of size more than 20 nm. Aneesh *et al.*[87] used Au nanoparticles as plasmonic nanomaterial in orgarnic SCs made of ITO/ MoO_3/P$_3$HT : PC$_{61}$BM/Al, and achieved 16% increase in short circuit current density while conversion efficiency improved up to 25%.

Researchers have demonstrated plasmon-enhanced photocurrent in different photovoltaics, including those based on CdSe[88], CdS[89] InP/InGaAsP[90], PbS[91] GaAs[92], InGaN/GaN[93], InGaAs/GaAs[84], *c*-Si[95], *a*-Si : H[96], organic semiconductors[97,98] such as polythiophene and copper pthalocyanine, and hybrid organic–inorganic devices such as DSSCs[99,100]. Al, Au and Ag nanoparticles have been explored as plasmonic nanomaterial, and Ag has the highest quality factor[101].

Conclusion

Incorporation of nanostructured materials in QDSSCs can significantly improve light absorption owing to large surface-to-volume ratio offered by them. Tuneable band gap and multiple exciton generation in QDs have opened up innumerable possibilities in high-efficiency SC

design. Nanostructured TiO_2 and ZnO are widely used as semiconducting material for the transport layer in QDSSCs. Though the efficiency obtained with TiO_2 is better than ZnO at present, the latter is gaining popularity as it has the advantage of higher electron mobility (200 cm^2/V/s) than the former (30 cm^2/V/s). Many structures of SCs have evolved based on QD sensitizers. Energy loss due to thermalization of hot charge carriers and sub-bandgap transmission can be addressed using tandem structures. A tandem structure of TiO_2/CdS/Cu–ZnS is reported to have an improved efficiency of 3.35%, which is 82% higher than TiO_2/CdS-based QDSSCs[71]. It is reported that cell efficiency increases by 600% with double layer of passivation compared to cells containing only CdTe. In core–shell structure, cooling of the hot carriers is slower, which helps in carrier multiplication and hence improves efficiency. Lai et al.[75] studied PbS core and CdS shell, and found four times higher efficiency than that obtained with simple PbS QDs coated with ZnS after deposition. $CdSe/(CdSe_xS_{1-x})_5/(CdS)_1$ core/shell QD-based QDSSCs are reported to have a maximum photo-conversion efficiency of 6.86% (ref. 76). An optically thick but physically thin structure of a SC is highly desirable. It can be achieved by means of plasmonic SCs, where light trapping mechanism is introduced in already designed cells. This review will be helpful to SC enthusiasts working on novel designs.

1. US Energy Information Administration, International Energy Outlook, 2010.
2. Zhang, Q. and Cao, G., Nanostructured photoelectrodes for dye-sensitized solar cells. *Nano Today*, 2011, **6**, 91–109.
3. Green, M. A. et al., Solar cell efficiency tables (version 37), *Prog. Photovolt.: Res. Appl.*, 2010, **19**, 84–92.
4. Bandara, J. and Weerasinghe, H. C., Efficient solid-state dye sensitized solar cells fabricated on a compact TiO_2 barrier layer preventing short-circuit current. *Sri Lankan J. Phys.*, 2004, **5**, 27–35.
5. Grätzel, M., Conversion of sunlight to electric power by nanocrystalline dye-sensitized solar cells. *J. Photochem. Photobiol. A: Chem.*, 2004, **164**, 3–14.
6. Halim, M. A., Harnessing sun's energy with quantum dots based next generation solar cell. *Nanomaterials*, 2012, **3**, 22–47.
7. Chakrapani, V., Baker, D. and Kamat, P. V., Understanding the role of the sulfide redox couple (S^{2-}/S_n^{2-}) in quantum dot-sensitized solar cells. *J. Am. Chem. Soc.*, 2011, **133**, 9607–9615.
8. Ellis, A. B., Steven, W. K. and Mark, S. W., Optical to electrical energy conversion. Characterization of cadmium sulfide and cadmium selenide based photoelectrochemical cells. *J. Am. Chem. Soc.*, 1976, **98**, 6855–6866.
9. Yu, J. et al., Quantum dot sensitized solar cells with efficiency over 12% based on tetraethyl orthosilicate additive in polysulfide electrolyte. *J. Mater. Chem. A*, 2017, **5**, 14124–14133.
10. Meng, K., Surolia, P. K., Byrne, O. and Thampi, K. R., Efficient CdS quantum dot sensitized solar cells made using novel Cu_2S counter electrode. *J. Power Sour.*, 2014, **248**, 218–223.
11. Meng, K., Surolia, P. K., Byrne, O. and Thampi, K. R., Quantum dot and quantum dot–dye co-sensitized solar cells containing organic thiolate–disulfide redox electrolyte. *J. Power Sour.*, 2015, **275**, 681–687.
12. Tian, J. and Cao, G., Semiconductor quantum dot-sensitized solar cells. *Nano Rev.*, 2013, **4**, 1–8.
13. Jun, H. K., Careem, M. A. and Arof, A. K., Efficiency improvement of CdS and CdSe quantum dot-sensitized solar cells by TiO_2 surface treatment. *J. Renew. Sustain. Energ.*, 2014, **6**, 023107.
14. Cheng, D.-C. et al., Improving Si solar cell performance using Mn : ZnSe quantum dot-doped PLMA thin film. *Nanoscale Res. Lett.*, 2013, **8**, 291.
15. Sfyri, G. et al., Composite ZnSe–CdSe quantum dot sensitizers of solid-state solar cells and the beneficial effect of added Na_2S. *J. Phys. Chem. C*, 2014, **118**, 16547–16551.
16. Singh, R. et al., Synthesis of lead sulphide nanoparticles for electrode application of dye sensitized solar cells. *Nanosci. Nanotechnol. Lett.*, 2014, **6**, 31–36.
17. Jean, J. et al., ZnO nanowire arrays for enhanced photocurrent in PbS quantum dot solar cells. *Adv. Mater.*, 2013, **25**, 2790–2796.
18. Hu, H. et al., Photodeposition of Ag_2S on TiO_2 nanorod arrays for quantum dot-sensitized solar cells. *Nanoscale Res. Lett.*, 2013, **8**, 1–7.
19. Hwang, I. et al., Improvement of photocurrent generation of Ag_2S sensitized solar cell through co-sensitization with CdS. *Appl. Phys. Lett.*, 2013, **103**, 023902–023902.
20. Jara, D. H. et al., Size-dependent photovoltaic performance of $CuInS_2$ quantum dot-sensitized solar cells. *Chem. Mater.*, 2014, **26**, 7221–7228.
21. Li, T., Lee, Y. L. and Teng, H., High-performance quantum dot-sensitized solar cells based on sensitization with $CuInS_2$ quantum dots/CdS heterostructure. *Energ. Environ. Sci.*, 2012, **5**, 5315–5324.
22. Wang, J. et al., Core/shell colloidal quantum dot exciplex states for the development of highly efficient quantum-dot-sensitized solar cells. *J. Am. Chem. Soc.*, 2013, **135**, 15913–15922.
23. Lu, Z. et al., One-step aqueous synthesis of grapheme–CdTe quantum dot-composed nanosheet and its enhanced photoresponses. *J. Colloid Interf. Sci.*, 2011, **353**, 588–592.
24. Zhang X. et al., Comparative cytotoxicity of gold–doxorubicin and InP–doxorubicin conjugates. *Nanotechnology*, 2012, **23**, 275103–275115.
25. Zaban, A. M. O. I. et al., Photosensitization of nanoporous TiO_2 electrodes with InP quantum dots. *Langmuir*, 1998, **14**, 3153–3156.
26. Taniguchi, S., Green, M. and Lim, T., The room-temperature synthesis of anisotropic CdHgTe quantum dot alloys: a 'molecular welding' effect. *J. Am. Chem. Soc.*, 2011, **133**, 3328–3331.
27. Feteha, M. Y. and Ameen, M., CdHgTe quantum dots sensitized solar cell with using of titanium dioxide nanotubes. *J. Power Energy Eng.*, 2013, **1**, 67–72.
28. Sudhagar, P. et al., Quantum dot-sensitized solar cells. In *Low-Cost Nanomaterials*, Springer London, 2014, pp. 89–136.
29. Tian, J. et al., Architectured ZnO photoelectrode for high efficiency quantum dot sensitized solar cells. *Energ. Environ. Sci.*, 2013, **6**, 3542–3547.
30. Perera, V. P. S., An efficient dye-sensitized photoelectrochemical solar cell made from oxides of tin and zinc. *Chem. Commun.*, 1999, **1**, 15–16.
31. Sayama, K., Sugihara, H. and Arakawa, H., Photoelectrochemical properties of a porous Nb_2O_5 electrode sensitized by a ruthenium dye. *Chem. Mater.*, 1998, **10**, 3825–3832.
32. Liu, Z. et al., Enhancing the performance of quantum dots sensitized solar cell by SiO_2 surface coating. *Appl. Phys. Lett.*, 2010, **96**, 233107-3.
33. Seol, M. et al., Novel nanowire array based highly efficient quantum dot sensitized solar cell. *Chem. Commun.*, 2010, **46**, 5521–5523.
34. Yu, Z. et al., Highly efficient quasi-solid-state quantum-dot-sensitized solar cell based on hydrogel electrolytes. *Electrochem. Commun.*, 2010, **12**, 1776–1779.

35. Fang, B. *et al.*, Facile synthesis of open mesoporous carbon nanofibers with tailored nanostructure as a highly efficient counter electrode in CdSe quantum-dot-sensitized solar cells. *J. Mater. Chem.*, 2011, **21**, 8742–8748.

36. Radich, J. G., Dwyer, R. and Kamat, P. V., Cu_2S reduced graphene oxide composite for high-efficiency quantum dot solar cells. Overcoming the redox limitations of S^{2-}/Sn^{2-} at the counter electrode. *J. Phys. Chem. Lett.*, 2011, **2**, 2453–2460.

37. Zhang, Q. *et al.*, Highly efficient CdS/CdSe-sensitized solar cells controlled by the structural properties of compact porous TiO_2 photoelectrodes. *Phys. Chem. Chem. Phys.*, 2011, **13**, 4659–4667.

38. Hossain, M. A. *et al.*, CdSe-sensitized mesoscopic TiO_2 solar cells exhibiting >5% efficiency: redundancy of CdS buffer layer. *J. Mater. Chem.*, 2012, **22**, 16235–16242.

39. Santra, P. K. and Kamat, P. V., Mn-doped quantum dot sensitized solar cells: a strategy to boost efficiency over 5%. *J. Am. Chem. Soc.*, 2012, **134**, 2508–2511.

40. Law, M. *et al.*, Nanowire dye-sensitized solar cells. *Nature Mater.*, 2005, **4**, 455–459.

41. Yang, P. *et al.*, Controlled growth of ZnO nanowires and their optical properties. *Adv. Funct. Mater.*, 2002, **12**, 323–331.

42. Xia, J. B. and Zhang, X. W., Electronic structure of ZnO wurtzite quantum wires. *Eur. Phys. J. B*, 2006, **49**, 415–420.

43. Quintana, M. *et al.*, Comparison of dye-sensitized ZnO and TiO_2 solar cells: studies of charge transport and carrier lifetime. *J. Phys. Chem. C*, 2007, **111**, 1035–1041.

44. Baruah, S. and Dutta, J., Hydrothermal growth of ZnO nanostructures. *Sci. Technol. Adv. Mater.*, 2009, **10**, 013001–18.

45. Singh, N. *et al.*, ZnO based quantum dot sensitized solar cell using CdS quantum dots. *J. Renew. Sustain. Energy*, 2012, **4**, 013110-10.

46. Yuan, Z. and Longwei, Y., CdSe–CdS quantum dots co-sensitized ZnO hierarchical hybrids for solar cells with enhanced photoelectrical conversion efficiency. *Nanoscale*, 2014, **6**, 13135–13144.

47. Eskandari, M., Ahmadi, V. and Kohnehpoushi, S., Improvement of ZnO nanorod based quantum dot (cadmium sulfide) sensitized solar cell efficiency by aluminum doping. *Phys. E*, 2015, **66**, 275–282.

48. Wang, X. *et al.*, Tandem colloidal quantum dot solar cells employing a graded recombination layer. *Nature Photoni.*, 2011, **5**, 480–484.

49. Grätzel, M., Photoelectrochemical cells. *Nature*, 2001, **414**, 338–344.

50. Chang, C. H. and Lee, Y. L., Chemical bath deposition of CdS quantum dots onto mesoscopic TiO_2 films for application in quantum-dot-sensitized solar cells. *Appl. Phys. Lett.*, 2007, **91**, 053503-3.

51. Bang, J. H. and Kamat, P. V., Quantum dot sensitized solar cells. A tale of two semiconductor nanocrystals: CdSe and CdTe. *ACS Nano*, 2009, **3**(6), 31467–31476.

52. Kongkanand, A. *et al.*, Quantum dot solar cells. Tuning photoresponse through size and shape control of CdSe–TiO_2 architecture. *J. Am. Chem. Soc.*, 2008, **130**, 4007–4015.

53. Chen, J. *et al.*, An oleic acid-capped CdSe quantum-dot sensitized solar cell. *Appl. Phys. Lett.*, 2009, **94**, 153115-3.

54. Gorer, S. and Hodes, G., Quantum size effects in the study of chemical solution deposition mechanisms of semiconductor films. *J. Phys. Chem.*, 1994, **98**, 5338–5346.

55. Thambidurai, M. *et al.*, Strong quantum confinement effect in nanocrystalline CdS. *J, Mater. Sci.*, 2010, **45**, 3254–3258.

56. Vogel, R., Hoyer, P. and Weller, H., Quantum-sized PbS, CdS, Ag_2S, Sb_2S_3, and Bi_2S_3 particles as sensitizers for various nanoporous wide-bandgap semiconductors. *J. Phys. Chem.*, 1994, **98**, 3183–3188.

57. Schaller, R. D. and Klimov, V. I., High efficiency carrier multiplication in PbSe nanocrystals: implications for solar energy conversion. *Phys. Rev. Lett.*, 2004, **92**, 18660-(1–16).

58. Lee, Y. K., Lee, H. and Park, J. Y., Tandem-structured, hot electron based photovoltaic cell with double Schottky barriers. *Sci. Rep.*, 2014, **4**, 4580-1–4580-6.

59. Meillaud, F. *et al.*, Efficiency limits for single-junction and tandem solar cells. *Sol. Energy Mater. Solar Cells*, 2006, **90**, 2952–2959.

60. Nattestad, A. *et al.*, Highly efficient photocathodes for dye-sensitized tandem solar cells. *Nature Mater.*, 2010, **9**, 31–35.

61. Nozik, A. J., Quantum dot solar cells. *Physica E*, 2002, **14**, 115–120.

62. Benisty, H., Reduced electron-phonon relaxation rates in quantum-box systems: theoretical analysis. *Phys. Rev. B*, 1995, **51**, 13281.

63. Nozik, A. J., Spectroscopy and hot electron relaxation dynamics in semiconductor quantum wells and quantum dots. *Ann. Rev. Phys. Chem.*, 2001, **52**, 193–231.

64. Bockelmann, U. and Bastard, G., Phonon scattering and energy relaxation in two-, one-, and zero-dimensional electron gases. *Phys. Rev. B*, 1990, **42**, 8947.

65. Dou, L *et al.*, Systematic investigation of benzodithiophene- and diketopyrrolopyrrole-based low-bandgap polymers designed for single junction and tandem polymer solar cells. *J. Am. Chem. Soc.*, 2012, **134**, 10071–10079.

66. You, J. *et al.*, A polymer tandem solar cell with 10.6% power conversion efficiency. *Nature Commun.*, 2013, **4**, 1446–1410.

67. Coffin, R. C. *et al.*, Streamlined microwave-assisted preparation of narrow-bandgap conjugated polymers for high-performance bulk heterojunction solar cells. *Nature Chem.*, 2009, **1**, 657–661.

68. Mühlbacher, D. *et al.*, High photovoltaic performance of a low-bandgap polymer. *Adv. Mater.*, 2006, **18**, 2884–2889.

69. Conibeer, G. *et al.*, Silicon quantum dot nanostructures for tandem photovoltaic cells. *Thin Solid Films*, 2008, **516**, 6748–6756.

70. Santra, P. K. and Kamat, P. V., Tandem-layered quantum dot solar cells: tuning the photovoltaic response with luminescent ternary cadmium chalcogenides. *J. Am. Chem. Soc.*, 2013, **135**, 877–885.

71. Lee, Y.-S. *et al.*, High performance of TiO_2/CdS quantum dot sensitized solar cells with a Cu–ZnS passivation layer. *New J. Chem.*, 2017, **41**, 1914–1917.

72. Vitoreti, A. B. F. *et al.*, CdTe and CdTe/CdSe core/shell aqueous soluble quantum dots-sensitized solar cell. In Proceedings of International Conference, University of Minho, Braga, Partugal, 2017.

73. Mora-Sero, I. *et al.*, Recombination in quantum dot sensitized solar cells. *Acc. Chem. Res.*, 2009, **42**, 1848–1857.

74. Guijarro, N. *et al.*, Uncovering the role of the ZnS treatment in the performance of quantum dot sensitized solar cells. *Phys. Chem. Chem. Phys.*, 2011, **13**, 12024–12032.

75. Lai, L. H. *et al.*, Sensitized solar cells with colloidal PbS–CdS core–shell quantum dots. *Phys. Chem. Chem. Phys.*, 2014, **16**, 736–742.

76. Selopal, G. S. *et al.*, Highly stable colloidal 'giant' quantum dots sensitized solar cells. *Adv. Funct. Mater.*, 2017, **27**, 1701468.

77. Atwater, H. A. and Polman, A., Plasmonics for improved photovoltaic devices. *Nature Mater.*, 2010, **9**, 205–213.

78. Green, M. A. and Pillai, S., Harnessing plasmonics for solar cells. *Nature Photon.*, 2012, **6**, 130–132.

79. Nelson, J., *The Physics of Solar Cells*, World Scientific Publishing Co Inc, London, 2003.

80. Hägglund, C. and Apel, S. P. L., Plasmonic near-field absorbers for ultrathin solar cells. *J. Phys. Chem. Lett.*, 2012, **3**, 1275–1285.

81. Hägglund, C. and Kasemo, B., Nanoparticle plasmonics for 2D-photovoltaics: mechanisms, optimization and limits. *Opt. Exp.*, 2009, **17**, 11944–11957.

82. Hägglund, C. and Apell, S. P., Resource efficient plasmon-based 2D-photovoltaics with reflective support. *Opt. Exp.*, 2010, **18**, A343–A356.

83. Westphalen, M. *et al.*, Metal cluster enhanced organic solar cells. *Sol. Energ. Mater. Sol. Cells*, 2000, **61**, 97–105.

84. Moulin, E. *et al.*, Photoresponse enhancement in the near infrared wavelength range of ultrathin amorphous silicon photosensitive devices by integration of silver nanoparticles. *Appl. Phys. Lett.*, 2009, **95**, 033505.

85. White, T. P. and Kylie, R. C., Plasmon-enhanced internal photoemission for photovoltaics: theoretical efficiency limits. *Appl. Phys. Lett.*, 2012, **101**, 073905-4.

86. Fleetham, T. *et al.*, Photocurrent enhancements of organic solar cells by altering dewetting of plasmonic Ag nanoparticles. *Sci. Rep.*, 2015, **5**, 14250-1–14250-9.

87. Aneesh, P. M. *et al.*, Enhancement in photovoltaic properties of plasmonic nanostructures incorporated organic solar cells processed in air using P3HT: PCBM as a model active layer. *Org. Photon. Photovolt.*, 2015, **3**, 64–70.

88. Konda, R. B. *et al.*, Surface plasmon excitation via Au nanoparticles in *n*-CdSe/ *p*-Si heterojunction diodes. *Appl. Phys. Lett.*, 2007, **91**, 191111-1–191111-3.

89. Zhao, W. W. *et al.*, Exciton-plasmon interactions between CdS quantum dots and Ag nanoparticles in photoelectrochemical system and its biosensing application. *Anal. Chem.*, 2012, **84**, 5892–5897.

90. Derkacs, D. *et al.*, Nanoparticle-induced light scattering for improved performance of quantum-well solar cells. *Appl. Phys. Lett.*, 2008, **93**, 091107-1–091107-3.

91. Kawawaki, T. *et al.*, Efficiency enhancement of PbS quantum dot/ZnO nanowire bulk-heterojunction solar cells by plasmonic silver nanocubes. *ACS Nano*, 2015, **9**, 4165–4172.

92. Nakayama, K., Tanabe, K. and Atwater, H. A., Plasmonic nanoparticle enhanced light absorption in GaAs solar cells. *Appl. Phys. Lett.*, 2008, **93**, 121904-1–121904-3.

93. Pryce, I. M. *et al.*, Plasmonic nanoparticle enhanced photocurrent in GaN/InGaN/GaN quantum well solar cells. *Appl. Phys. Lett,*, 2010, **96**, 153501-3.

94. Lu, H. F. *et al.*, Plasmonic quantum dot solar cells for enhanced infrared response. *Appl. Phys. Lett.*, 2012, **100**, 103505-4.

95. Pillai, S. *et al.*, Surface plasmon enhanced silicon solar cells. *J. Appl. Phys.*, 2007, **101**, 093105-8.

96. Gusak, V., Kasemo, B. and Hagglund, C., High aspect ratio plasmonic nanocones for enhanced light absorption in ultrathin amorphous silicon films. *J. Phys. Chem. C*, 2014, **118**, 22840–22846.

97. Westphalen, M. *et al.*, Metal cluster enhanced organic solar cells. *Sol. Energy Mater. Solar Cells*, 2000, **61**, 97–105.

98. Morfa, A. J. *et al.*, Plasmon-enhanced solar energy conversion in organic bulk heterojunction photovoltaics. *Appl. Phys. Lett.*, 2008, **92**, 013504.

99. Yin, X., Que, W. and Shen, F., Improvement of the performance of dye sensitized solar cell using ZnO nanorods array deposited with Ag nanoparticles as photoanode. *J. Sol–gel Sci. Technol.*, 2012, **63**, 279–285.

100. Muduli, S. *et al.*, TiO_2-Au plasmonic nanocomposite for enhanced dye-sensitized solar cell (DSSC) performance. *Sol. Energ.*, 2012, **86**, 1428–1434.

101. Catchpole, K. R. and Polman, A., Design principles for particle plasmon enhanced solar cells. *Appl. Phys. Lett.*, 2008, **93**, 191113-3.